All-in-One Print: Designing and 3D Printing Dynamic Objects Using Kinematic Mechanism without Assembly

All-in-One Print: Designing and 3D Printing Dynamic Objects Using Kinematic Mechanism Without Assembly

Jiaji Li
Zhejiang University
lijiaji@zju.edu.cn

Mingming Li
Zhejiang University
mingmingli@zju.edu.cn

Junzhe Ji
Zhejiang University
jjunzhe@zju.edu.cn

Deying Pan
Zhejiang University
deyingp2@zju.edu.cn

Yitao Fan
Zhejiang University
ytfan@zju.edu.cn

Kuangqi Zhu
Zhejiang University
kuangqizhu@zju.edu.cn

Yue Yang
Zhejiang University
yang_yue@zju.edu.cn

Zihan Yan
MIT Media Lab
yzihan@media.mit.edu

Lingyun Sun
Zhejiang University
sunly@zju.edu.cn

Ye Tao
Hangzhou City University
taoye@zucc.edu.cn

Guanyun Wang*
Zhejiang University
guanyun@zju.edu.cn

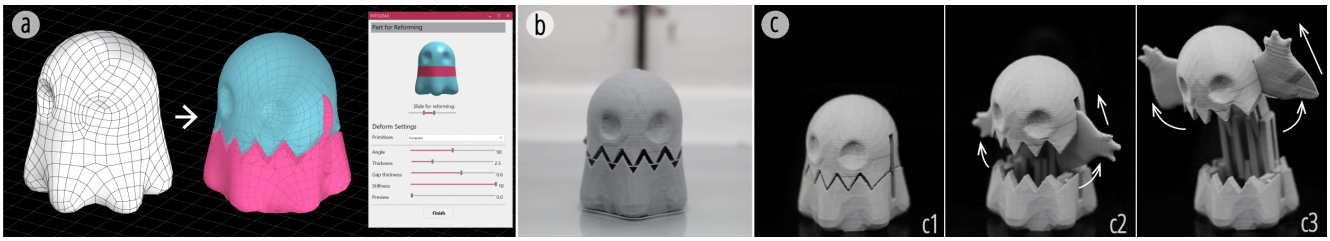

Figure 1: Reforming a solid ghost model through All-in-One Print: (a) importing a rigid ghost model and customizing deformation components integrated inside its body; (b) printing the ghost with Arch-printing and Support-bridges. (c)The final print has multiple primitives with a body that can be stretched to 2.5 times its length and two rotatable arms.

ABSTRACT

The field of Human-Computer-Interaction (HCI) has been consistently utilizing kinematic mechanisms to create tangible dynamic interfaces and objects. However, the design and fabrication of these mechanisms are challenging due to complex spatial structures, step-by-step assembly processes, and unstable joint connections resulting from the inevitable matching errors within separated parts. In this paper, we propose an integrated fabrication method for one-step FDM 3D printing (FDM3DP) kinematic mechanisms to create dynamic objects without additional post-processing. We describe the Arch-printing and Support-bridges method, which we call All-in-One Print, that compiles given arbitrary solid 3D models into printable kinematic models as G-Code for FDM3DP. To expand the design space, we investigate a series of motion structures (e.g., rotate, slide, and screw) with multi-stabilities and develop a design tool to help users quickly design such dynamic objects. We also demonstrate various application cases, including physical interfaces, toys with interactive aesthetics and daily items with internalized functions.

CCS CONCEPTS

• **Human-centered computing** → Human computer interaction (HCI); Interaction devices.

KEYWORDS

Fabrication, Prototyping/Implementation

ACM Reference Format:
Jiaji Li, Mingming Li, Junzhe Ji, Deying Pan, Yitao Fan, Kuangqi Zhu, Yue Yang, Zihan Yan, Lingyun Sun, Ye Tao, and Guanyun Wang. 2023. All-in-One Print: Designing and 3D Printing Dynamic Objects Using Kinematic Mechanism Without Assembly. In *Proceedings of the 2023 CHI Conference on Human Factors in Computing Systems (CHI '23), April 23–28, 2023, Hamburg, Germany.* ACM, New York, NY, USA, 15 pages. https://doi.org/10.1145/3544548.3581440

*Corresponding Author: Guanyun Wang, guanyun@zju.edu.cn

CHI '23, April 23–28, 2023, Hamburg, Germany

ACM ISBN 978-1-4503-9421-5/23/04…$15.00
https://doi.org/10.1145/3544548.3581440

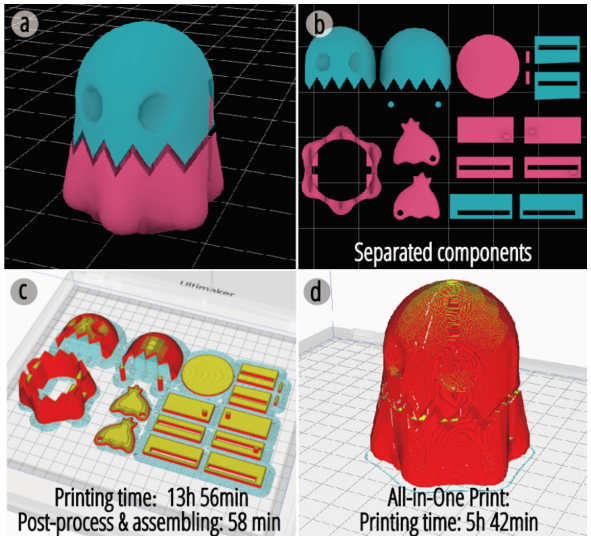

Figure 2: (a) The virtual model of a ghost with mechanical components inside; (b,c) Eighteen separated components that require assembling with the conventional method; (d) The same ghost printed entirely with All-in-One Print method.

1 INTRODUCTION

From creating input devices [15, 18] to presenting tangible information [19, 20], from interactive toys [24] to shape-changing installations [13], the field of HCI has been consistently utilizing kinematic mechanisms [46] to create tangible dynamic interfaces and objects. However, for FDM3DP, the design and fabrication of these mechanisms can be challenging due to their complex three-dimensional structures and step-by-step assembly processes. In detail, the manufacturing of parts increases the production time, as well as the difficulty of assembly of kinematic mechanisms resulting from inevitable matching errors within separated parts (Figure 2b, c).

To response, integrated fabrication has been introduced to the HCI community to fabricate complex mechanical structures by minimizing post-processing and optimizing fabrication iteration. For example, LaserOrigami [49] provides a technique to laser cut flat sheets into 3D structures without assembly; some studies utilize additive manufacturing technology to 3D print classical mechanisms without post-processing efforts, i.e., spring [9, 39, 54], linkages [12, 14, 36], popup hinges [22], self-locking [4, 34], telescoping [41] and joints [3, 45]. However, most of them require advanced printers (SLA, SLS) and strict forward design workflow, which limit their accessibilities and possibilities for inverse-engineering objects in HCI.

Recent developments based on consumer FDM 3D printers, i.e., G-code controlled bridging printing techniques [11, 43, 44, 47, 52], allow makers, designers, and HCI researchers to produce integrated structures with multiple mechanisms for customization and prototyping. However, the adhesion issues we identified often affect the reliability and usability of these structures due to (1) improper scales of gaps reserved between components, resulting in mismatches with printer accuracy; (2) overhang polymers sinking and fusing with layers beneath (Figure 3a4, c); and (3) unremovable supports preventing flexibility (Figure 5b3).

To address these challenges, we have developed an optimized *Arch-printing* (Section 3.1) and *Support-bridges* (Section 3.2) method that enables one-step FDM 3D printing without additional post-processing, as seen in Figure 2d. This folded structure significantly reduces printing time and extra manual effort.

To better introduce the kinematic mechanisms to the HCI community and enable its design space for HCI users, we have integrated a series of motion structures (e.g., rotate, slide, and screw) with diverse stabilities into an inverse design process. We hope that this will expand access and enable the exploration of what more the objects with kinematic mechanisms can be.

In summary, our primary contributions include the following:

- Methods and principles including *Arch-printing* and *Support-bridges* for FDM3DP folded objects with kinematic mechanisms including rotating, sliding, and screwing.
- A pipeline to support different users with an accessible design process and automatic G-code generation by minimizing post-processing and improving the robustness of joints.
- Application examples to demonstrate the accessibility of All-in-One Print for customized objects.

2 RELATED WORK

2.1 Digital Fabrication and Interactive Design of Flexible Structures

The use of digital fabrication technology, such as 3D printing and laser cutting, to create shape-changing flexible interfaces, daily objects, and artifacts are of increasing interest in the HCI community. Some of the research projects utilize the properties of materials to 3D print objects whose shapes can vary with temperatures [31, 39, 40, 55] or electric[56]. Some explore metamaterials [2, 7, 30, 37, 53] to control the elasticity of 3D-printed objects as a whole, and other work proposes different mechanisms to make 3D-printed or laser-cut objects flexible and easy to deform. These mechanisms include 3D printed joints [3, 45], linkages [10, 12, 14, 36], hinges [22], truss structures [8, 13, 32], grid structures [26], and compliant mechanisms [9, 16, 54].

In general, fabricating flexible structures requires advanced fabrication devices [3] or involves design processes that are too complex and challenging for novice users [32]. Researchers have developed interactive design tools to help novices fabricate flexible structures using certain mechanisms: Ondulé [9] and Kinergy [54] allow beginners to create helical springs within 3D models for kinetic motions and energy, which are printable with FDM printers. Mechanism Perfboard [10] combines an augmented reality system to help users design and fabricate linkage mechanisms. We have developed a design tool to help users quickly create a G-code file of folded models, which is auto-generated from imported 3D models, and ready to be 3D printed.

2.2 Integrated Fabrication of Functional Objects

Manual assembly is often required after all the parts are 3D printed or laser cut to fabricate functional objects consisting of multiple

units or various components. This process typically requires knowledge of mechanisms and can be time-consuming. Also, the precision of the assembly is often compromised. Previous research has demonstrated methods to assist structural design and assembly. For laser cut structures and models, assembler3 [28], autoAssembler [29], FoolProofJoint [23], and Roadkill [1] explore the interfaces and algorithms to provide guides for assembling laser cut plates into 3D models.

Researchers have also proposed more integrated firmware and fabrication pipelines to simplify manufacturing, including assembling 3D-printed objects. LaserFactory [21] presents an assembly-free workflow that uses a laser cutter as a multifunctional platform for making functional devices. Integrated fabrication improves the overall process of making practical objects and lowers the threshold of novice users. Our work integrates complicated kinematic mechanisms into one-step FDM 3D printing without requiring manual post-processing.

2.3 Advanced 3D Printing Methods with FDM Printers

Recently, researchers in the field of HCI have manipulated various 3D printing parameters (e.g., printing speed, fan speed, and nozzle temperature) to achieve different printing results and applications. These parameters are typically adjustable in the slicer software and are written into G-code files generated by the software. Many works have demonstrated how to control these parameters for printing optimization [11, 38] or to print out unique 3D structures [25], even soft fabrics [6]. Jiang et al. propose a support generation method to reduce support material and enable long bridge printing [11]. Pieri et al. have evaluated the effect of temperature, extrusion rate multiplier, and fiber orientation on shape-memory polymers' fixing and recovery ratios [25]. Mitropoulou et al. present a design method for 3D printing complex shell surfaces, which are non-planar layered [17]. 3D Printed Fabric [33] explores the fabrication of flexible woven textiles by controlling the movement of the print header. In contrast, DefeXtiles [6] 3D prints soft textiles through a study of printing parameters, and Extruder-Turtle [5] showcases an open-source library that can generate G-code files for 3D printing textiles, textured surfaces, and string-art sculptures. Desktop Electrospinning [27] develops a 3D printer to create fibers using melt electrospinning technology.

In addition to 3D printing simple bridge structures or textiles, more design space and potential applications can be achieved by controlling parameters. This paper presents a novel approach to bridge printing to create support within multi-component 3D models.

3 ALL-IN-ONE PRINT METHOD

3.1 Arch-printing

In conventional FDM printing, the layer-by-layer printing process requires a solid flat platform and necessary support structures. However, there is some tolerance due to the inherent toughness of the material and the cooling process after extrusion, allowing unsupported horizontal filaments to resist gravity within a short distance. This material property allows for bridging-based printing [43], which reinforces overhang structures and increases the limit of the horizontal span of the overhang.

However, the overhang is strictly limited in printing distance. For example, as shown in Figure 3a, using the standard printing method to print a 50mm-long bridge will result in 1.7mm of underside sinking, causing the mechanism to be unfunctional (Figure 3a3, a4).

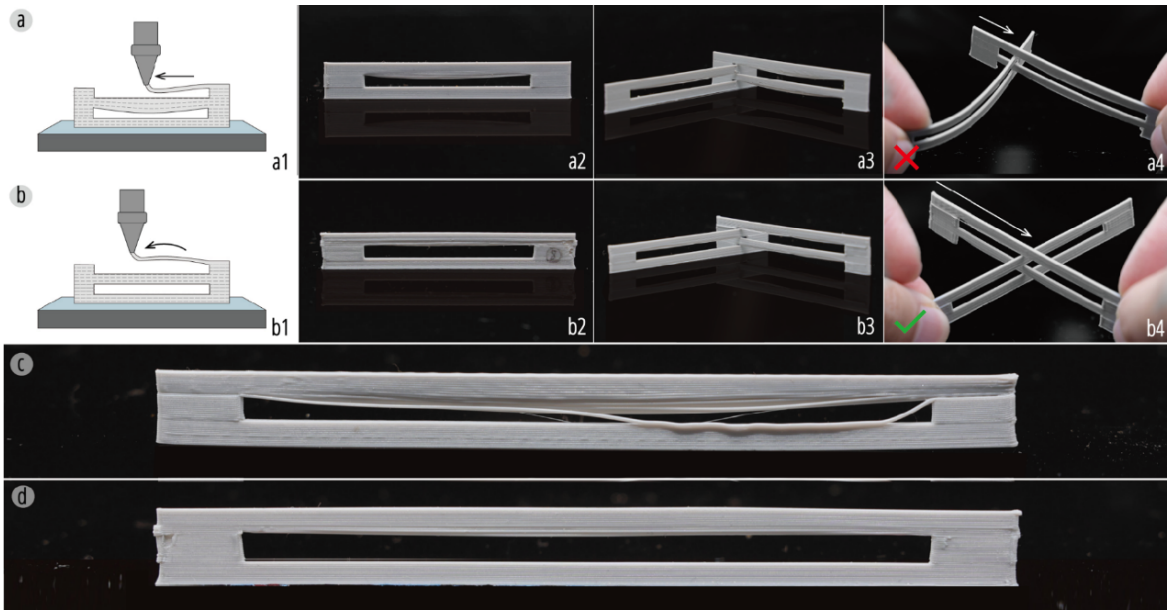

Figure 3: (a) Conventional 3D printed bridges of 50mm long and stuck result;(b) Arch-based 3D printing concept and slidable prints; (c, d) Compare two prints with a standard slicer and our method.

As a result, printing components with slide motion in the assembled state is at risk of compromised features.

Thanks to the G-code manipulation, we can perform *Arch-printing*, which relies on z-axis translation within a model slicing plane. The vertically undulating printing path allows the filament to cool and solidify in the sinking process, correcting the bias caused by gravity. To prevent hanging-down polymers, the first layer of arch printing is designed to be slightly arched even after solidification. A linear regression algorithm (Section 3.1.1) is used to gently iron out the arched layers in the 2-5 layers that follow, making them horizontal. To showcase our contribution, Figure 3d shows an 80 mm long *Arch-printing* result compared to the conventional bridging method (Figure 3c).

3.1.1 Arch Fitting Algorithm. Strategy for *Arch-printing*: In printing bridges, our method manipulates the printer to move upwards at the beginning and then downwards to the original altitude at the end, following a predetermined movement profile. This compensates for the sinking effect of the printed material. If the printing speed is slower than 30mm/s, the printed part can quickly solidify and self-support against gravity. Additionally, we use G-code commands to pause the printing for several seconds after the bridge layer is printed, ensuring that the base layer of the arch is solid.

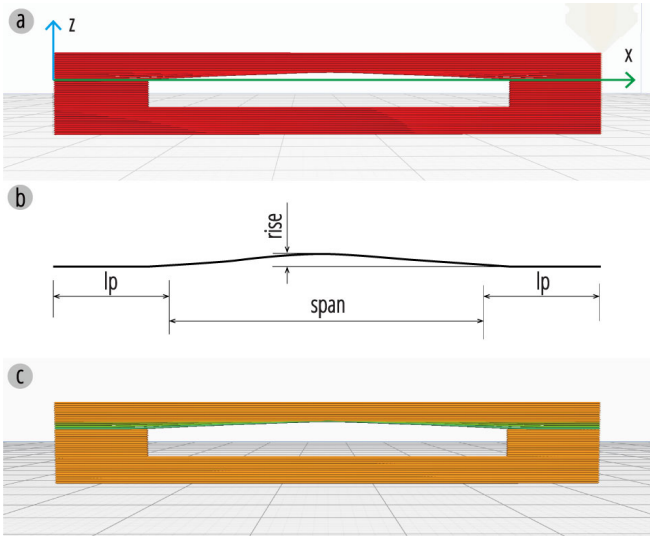

Figure 4: (a) The coordinate system to represent the arch curve by functions;(b) A basic model of the arch bridge with parameters; (c) Final preview of printing path with high arch-rise (green) to flat (orange).

To make a more defined expression, we build a basic model to describe our method. As shown in Figure 4a, a single bridge consists of two flat parts: the support pillars and the curved arch. The length of the arch along the X-axis is referred to as the span, and the height along the Z-axis is referred to as the rise (Figure 4b). By setting up a coordinate system in Figure 4a, we represent the arch curve using a set of convex functions. For example, using a sine function, we can calculate the height of the printer based on the distance it has covered on the X-axis:

$$Z(x) = \begin{cases} 0, & x \ \ l_p \ \ or \ \ x \ \ \ l_p + s \\ r \sin \frac{s}{\pi} \left(x - l_p\right), & l_p \ \leq x \leq \ l_p + s \end{cases} \quad (1)$$

Where r is the rise, s is the span, and l_p is the width of the pillars. Besides, we also apply some monotonic functions like *arctangent* and mirror them to get the entire arch curve with $x = l_p + \frac{s}{2}$ as the axis of symmetry:

$$Z(x) = \begin{cases} 0, & x \ \ l_p \ \ or \ \ x \ \ \ l_p + s \\ r \frac{4}{\pi} \tan^{-1} \frac{2}{s} \left(x - l_p\right), & l_p \ \leq x \leq \ l_p + \frac{s}{2} \\ r \frac{4}{\pi} \tan^{-1} \frac{2}{s} \left(l_p + s - x\right), & l_p + \frac{s}{2} \ \leq x \leq \ l_p + s \end{cases} \quad (2)$$

To generate the first layer of the bridges, we use the equations above. To create a smooth transition from the first arch layer to the first flat layer, we decrease the curvature layer by layer. In detail, we sample m points on the first arch layer and the first flat layer with the same X-coordinate. Next, we connect the corresponding points of the two curves and obtain m lines. Then, we divide each line into n segments with $n-1$ dividing points $p_{i1}, \ p_{i2}, \ldots, p_{in-1}, i = 1, 2, \ldots, m$.Finally, we interpolate the jth points of m lines into $n-1$ new curves:

$$Curve\,(j) \leftarrow Interpolate\left(p_{1j}, \ p_{2j}, \ldots, p_{mj}\right), j = 1, 2, \ldots, n-1$$

All the curves constitute the intact arch bridges with the curvatures decreasing from the bottom to the top (Figure 4c).

3.1.2 ***Printing test with multiple parameters.*** To better understand the effect of different printing parameters on the final result, we conducted a series of printing tests to determine the optimal parameters for *Arch-printing*. All tests were performed by printing a sample sheet with PLA at a temperature of 210°C and a layer height of 0.20 mm. The results showed that the arch function, arch rise, and the number of arch layers had the most significant impact on the final print quality. By carefully selecting these parameters, we were able to achieve smooth, horizontal bridges with minimal sinking.

Arch Functions: We tested various arch functions, including sine, parabolic, logarithm, arctangent, and hook functions. Among these, the arctangent function is most effective due to its relatively smooth and steady curvature with 3-5 points interpolated on the arch curves. In contrast, the asymmetry and different curvatures of other functions cause sinking in the rising and descending stage. This led to flexible and bending strands in the rising stage, joined by fast and strong downward pressure in the descending stages. Additionally, the results of the symmetric functions showed very little difference.

Arch Layers: The number of arch layers can slightly influence the results. When fewer than four layers exist, the curvature between layers can vary significantly, reducing the adhesion and support force between adjacent strands. On the other hand, having more than eight layers can cause the printer to move the top of the arch back and forth, which can help the strands sink. Based on our testing, we have found that 4-6 layers of arch typically perform as expected. In most cases, we use five layers as a standard.

Arch Rise: Arch rise is a critical parameter for arch printing. A short arch rise may not provide enough resistance to gravity, while a tall arch rise can stretch the strand, making it too soft to maintain its shape. We tested four groups of samples with spans

Table 1: Results of arch printing with different parameters.

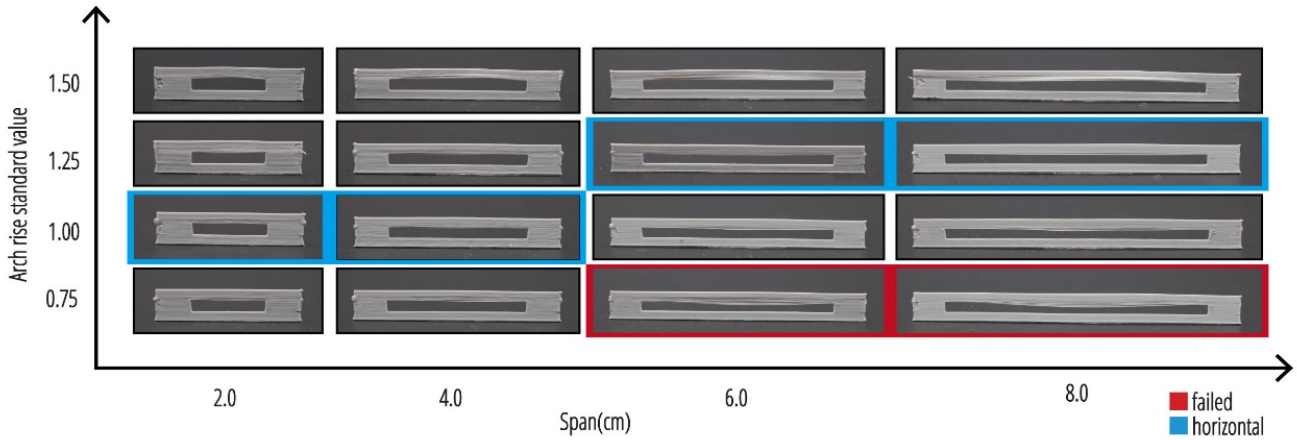

ranging from 2 cm to 8 cm, and for each group, we printed multiple samples with arch rises ranging from 0.2 mm to 2.0 mm. The results generally met our expectations, showing that the appropriate arch rise falls within a specific range and increases as the span length increases. To make the expression of arch rise more consistent, we defined a standard arch rise of 1.0 for each span length. For example, our tests showed that an arch rise of 0.8-1.0 mm worked best for a 4 cm span bridge. Therefore, we set 0.8mm as the standard arch rise of 1.0 for a 4cm span bridge. Table 1 shows part of our results. An arch rise of 0.75-1.0 can cause the bridge to sink slightly, providing a larger fraction of the gap, while an arch rise of 1.0-1.5 can cause the bridge to arch upward, providing more space in the gap. In practice, we typically select an arch rise of 1.0-1.2.

3.2 Support-bridges for replacement of support

In a conventional layer-by-layer printing strategy, separate components not attached to the platform require extensive support from the bed to its bottom. These supports can be crucial for flexibility in integrated printing, as they cannot be removed in enclosed spaces. Bridging or arch-printed filaments can be used as an alternative to support in such situations. In particular, by attaching several bridging-printed filaments to walls (Figure 5 c2), the first layer of grey parts can be bridging-printed again above them. A single strand of *Support-bridge* can be easily pulled off (with a force of less than 0.4 N), while a 2 mm×2 mm interlocking structure (consisting of the void of the structure highlighted in blue and the joint highlighted in red, in Figure 5) support more than 5 kg weight. Additionally, the compliance of bridging filaments minimizes their impact on subsequent motions. Arch-printing (Section 3.1) can be used in large-scale objects with longer bridges in conjunction with these support-replacement filaments to produce high-quality prints.

3.2.1 Load calculation for generation of Support-bridges. For *Support-bridges*, we have defined the following five principles to

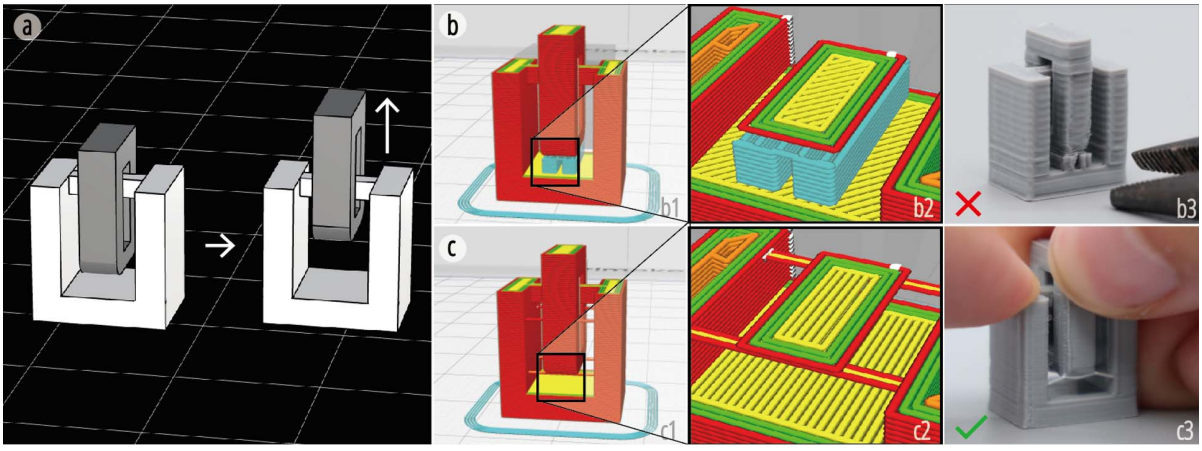

Figure 5: (a) A tiny sample of inter-locked slide motion ready for printing; (b) Conventional method with support barely removable; (c) *Support-bridges* method result which can be easily pulled off with motions.

create a more compatible strategy that aligns with G-code logic and user experience:

- P1. Layer-by-layer printing sequence without conflict with the existing G-code of other objects.
- P2. Generated with walls on both sides as pillars.
- P3. Sufficient toughness to support the load of objects between the bridges.
- P4. Non-linear arrangement to avoid shaking of objects during the printing process (Figure 6c).
- P5. Minimized the number of bridges for easy removal by manual pulling-off.

P1 allows for compatibility with conventional printers, while P2 and P3 ensure the generated bridges and objects are printable. P4 meets users' requirements for high-quality fabrication with minimal manual intervention (P5).

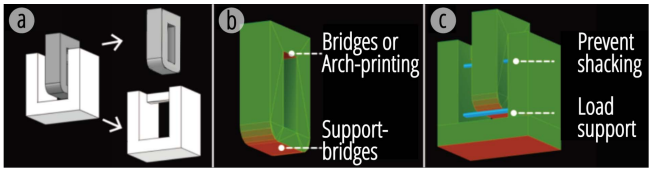

Figure 6: (a)Dispatched components for analysis; (b) red-marked parts for special printing strategy; (c) the Support-bridges added model ready for printing.

In specific, take the prototype in Figure 5a as an example. The algorithm to automatically generate *Support-bridges* is as follows: Firstly, we split the disjoint mesh to analyze a single component (Figure 6a). Then, with all the separated faces, we calculate the angle of their normal vectors downwards: the closer to the vertical, the more difficult it is to print. In general, they are marked as red (hard to print) to green (well-printable) in Figure 6b. As such, If the red part is connected to the completely green part at both ends (Figure 6b top), it is ideal to be printed by bridging or arch printing (Section 3.1). Otherwise, the part of the load must be supported by *Support-bridges*. With the initial setting, two bridges are added to both sides of the red area to help the bottom layer be well-printed. After that, the rest of the bridges are generated due to the load and size of the rest parts.

The calculation of load is as follows: Starting from the red section. The algorithm slices the component upward horizontally. For every 2cm, the *Support-bridges* will be added through centroids of sliced geometries, which consist of non-linear stabilization to prevent objects from shaking during the printing process. In this procedure, if one layer is connected with another vertical green surface, the rest of the load is assumed to be afforded by that. Otherwise, the whole will be sliced and calculated. The sum of all layers is the required load, which *Support-bridges* need to afford. According to the fabrication experience, each filament bridge can sustain a weight of 6g, and the final amount is calculated accordingly. Subtracting the amount for initialization and the amount to prevent shaking, the rest are added at the bottom to ensure the object is printable.

Table 2: Tensile strength scenarios and results.

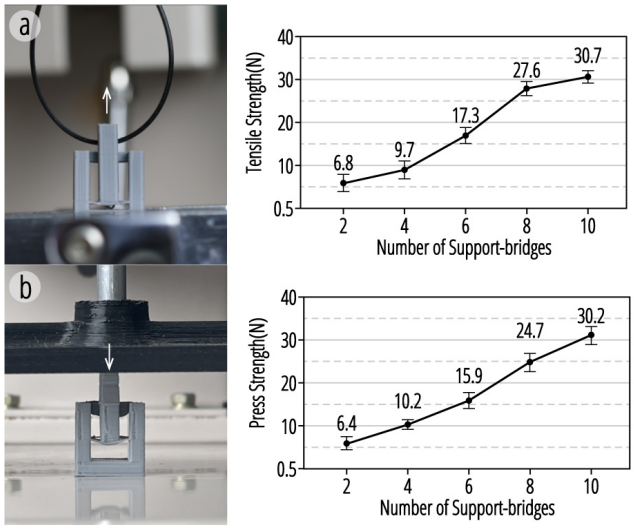

3.2.2 Tensile Strength. To verify the strength of the *Support-bridges* with our printing method, we tested their break load using a standard print sample. The sample is similar to the structure shown in Figure 6, consisting of the base and the overhang. These parts are connected by different numbers of aligned and evenly spread bridges. The testing equipment contains a force meter fixed on a vertical test stand. The base of the sample is clamped onto the bottom of the stand, while the top overhanging structure is attached to the force meter using a hook. Then, the force meter is cranked up until the *Support-bridges* break entirely, and the peak force is recorded.

4 EXAMPLE MECHANICAL MOTIONS

In this section, we finished multiple mechanical examples to introduce the design space of All-in-One Print. One-degree-of-freedom motions (Section 4.1) are primary features included in our design tool. In contrast, haptic stabilities (Section 4.2) and other extended structures with multi-directional deformation (Section 4.3-4.5) are specifically designed and generated. We demonstrate the extensibility of All-in-One Print in this section with a range of simple to complicated structures.

4.1 Fundamental motion primitives

The primary purpose of All-in-One Print is to print objects with integrated motion. In this section, we leverage three classic motion primitives. Each is a kinematic pair consisting of two components (red and white), all single-degree-of-freedom kinematic pairs. Their initial printed states are all 30 mm×30 mm×30 mm cubes to compare their motion capabilities easily.

4.1.1 Rotate. As shown in Figure 7a, the rotational motion is demonstrated using a *revolute joint*. In conventional 3D printing, each printed layer remains flat in solid objects. However, using our method, arch-printed bridges can be printed as a 30 mm-long cylinder that crosses the whole cube. In the printed cube, two parts are

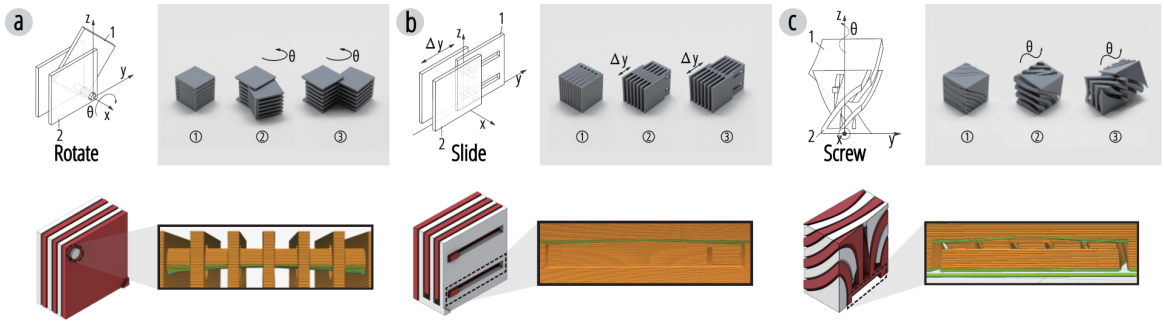

Figure 7: All-in-One Print primitives with (a) arch printed shaft through the whole cube;(b) arch printed slider for well-reserved gap; (c) arch printed bar connecting four parts.

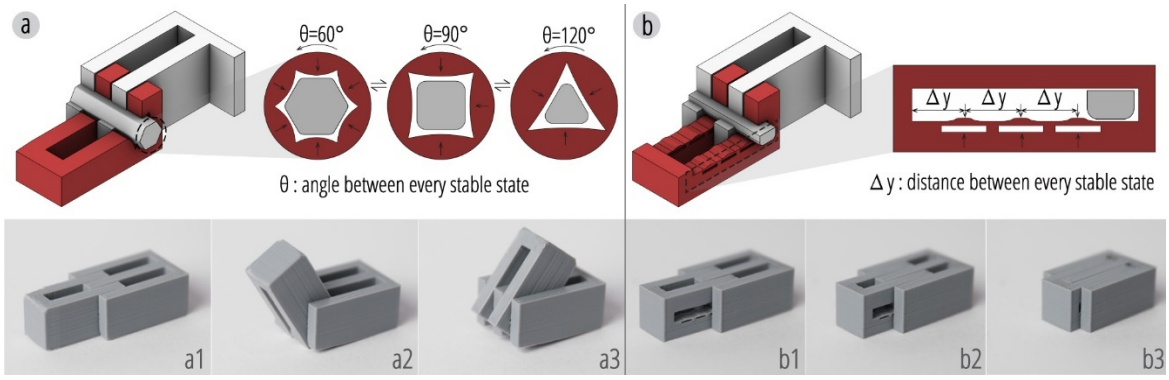

Figure 8: Multi-stable design for the motion of (a)slide and (b)rotate.

separated but locked together and cannot be pulled apart without breaking.

4.1.2 Slide. *The prismatic joint* is the most classic one-degree-of-freedom pair, which constrains the motion of two bodies to slide along a common axis (Figure 7b). As introduced in Section 3.1, arch printing creates horizontal and neat gaps in Figure 7b, which enable smooth sliding motion. In the first state, the joint can be stretched to 1.8 times the length of the cube sides. It also works as a compress primitive in the third state. Additionally, double tracks are designed for parallel movement.

4.1.3 Screw. Compared to planar slicing, a spirally divided cube is designed with spiral interlocking connections between the red and white parts (Figure 7c). The screw joint is a combination of both rising and rotating simultaneously, and it can convert the direction of input motion. As the red part rotates, the spiral surface between the two parts changes the torsional force into frictional force and upward thrust, pushing the white and red parts apart.

4.2 Multi-stability

The joints in Section 4.1 are designed without considering friction due to the gaps reserved between components to prevent fusing. However, using *Arch-printing* also enables All-in-One Print of multi-stable structures. In this section, we leverage the multi-stability of rotating and sliding motions and integrate them into the parametric design system.

To enable multi-stable rotational movement, we redesign the contact surface of the shaft-hole to be a polygon column (Figure 8a). The number of sides of the polygon determines the number of stable states. By tuning the arch *rise standard value* to -0.25 (Table 1), we can achieve inverted arches for multi-stability control on top of 60°and 120° polygons.

In the sliding joint, conventional bulges are used to control motion (Figure 8b), but they are prone to wear and tear after only a few uses. In our design, when the gray shaft is above the bulges, they are depressed. As the shaft passes over the bulges, they spring back and hold the shaft in place, providing stability and increasing the lifetime of the joint.

4.3 Expandability

One significant challenge for printing large-size objects is the limited size of the printer platform. All-in-One Print overcomes this challenge by integrating multiple primitives into a single object. For example, in Figure 9, a rectangle is printed with a double track integrated inside, which expands the capabilities of the fundamental slide primitive. This stretchable structure is also used in the design for the vertical stretch of the ghost in Figure 1.

However, planar motions do not fully utilize the three-dimensional fabrication of FDM printers. Using rotatable joints

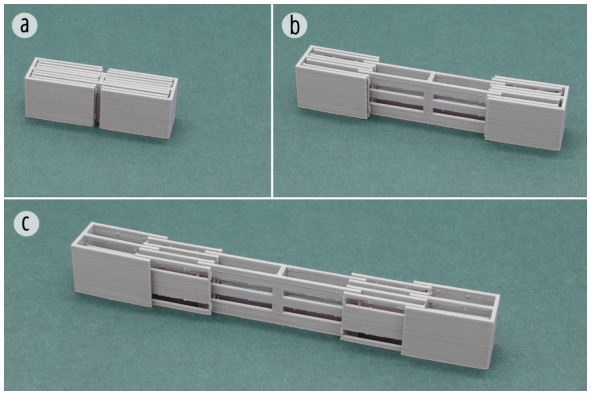

Figure 9: An expanded sample stretchable to 2.5 times of its initial length.

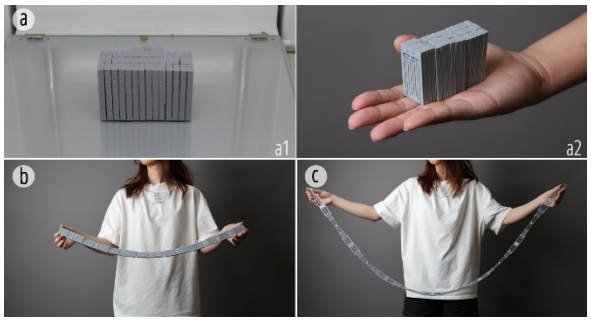

Figure 10: A 7×5×2.6 cm rectangle printed of hand-size (a), which can be rotated to human arm span (b) and stretched to the length of a human height(c).

to connect every two parts, a 7x5x2.6 cm rectangle is designed and printed in its entirety in Figure 10. The integrated components are supported by *Support-bridges* which can be easily removed by rotating and stretching. In its initial state, the structure is palm-size (7cm), but it can be opened up to arm-length (70 cm) and further stretched to human height (170 cm). Using approximate calculations, a printer with a 20 cm square printing platform can fabricate a chain-like structure that can reach three floors in height.

4.4 Ball joints

While none-assemble ball joints have been successfully fabricated using SLS printers by Calì et al. [45], desktop FDM printers still face limitations and challenges in fabricating such structures. Joining the parts of ball joints together relies primarily on the plastic deformation of the material. Once the attachment is successfully made, the opening of the socket inevitably becomes more prominent, undermining the secure connection. However, with the help of *Support-bridges* (Figure 11a, structures highlighted in blue), we can print several in-place ball joints within a single job, resulting in exceptional mobility compared to conventional methods to be customized to fit different needs. Figure 11 shows joints with diameters of Ø 6mm on the wrist, Ø10 mm on the elbow, and Ø14 mm on the shoulder, all with varying numbers of *Support-bridges*, which

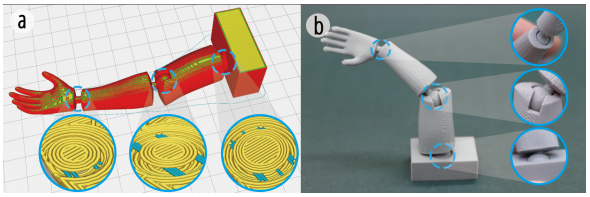

Figure 11: (a) G-code displayed with blue *Support-bridges* on every ball joint; (b)Printed arm with close-up details on ball joints.

can be easily removed by twisting and do not leave any uneven friction behind.

5 SOFTWARE PIPELINE

Overall, our system primarily contributes to the G-code generation of *Arch-printing* and *Support-bridges*, along with a simple design tool for the most basic motions. Section 5.1 introduces this design process from the perspective of different users. After that, Section 5.2 details the analysis and G-code generation using our specific method for print-at-one-go results. All the pipeline is built-up for the off-the-shelf FDM printer (Ultimaker S3) with Polymax PLA material of average elasticity and rigidity.

5.1 Kinetic design

To obtain a well-printable kinetically object for All-in-one printing, we have developed a software pipeline for users from novices to experts, from simple modifications using a design tool (Section 5.1.1) to more complex DIY design with guidance (Section 5.1.2).

5.1.1 Modification design tool for solid models. For novice users who are not familiar with kinematic designing and virtual modeling, we have developed a parametric platform using Grasshopper [42]. Figure 13 shows the function and design tool for All-in-One Print. In the design system, we have simplified the complicated dividing and interlock designing process using basic motions (section 4.1). Our design tool consists of three steps: model input, model dividing, and primitives customizing.

Firstly, when a solid virtual 3D model is input (Figure 14a), the system simplifies the model into a quad mesh, with the density of the mesh suitable for remodeling using Boolean operations. Then, by using the sliding bars on both sides and adjusting the angle, the user could preview the reformed area on the main interface in real-time (Figure 14b).

With the selection of primitives (Figure 14c), the part is divided into the default number of slices. The user can then customize the thickness of each slice using the Thickness slider (Figure 14d), which adjusts the number of slices and the gaps between them. Multiple slices help to stabilize the motion during manual deformation. The user can also control the range of motion using the Range slider (Figure 14e). Finally, the user can preview the finished model and choose a state for printing (Figure 14f). After completing one workflow, the remaining part can be selected and reformed again for additional deformation. After five cycles of reformation, the dinosaur is designed with a compressible neck and tail, together with four rotatable feet for integrated printing.

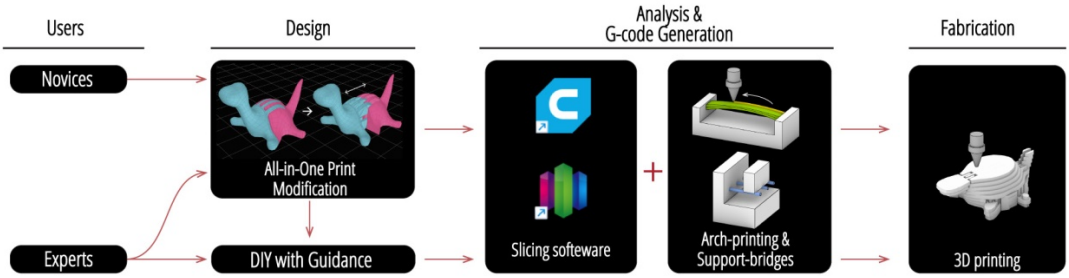

Figure 12: Pipeline for different users.

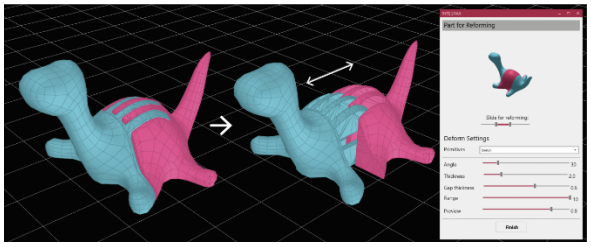

Figure 13: All-in-One Print interface.

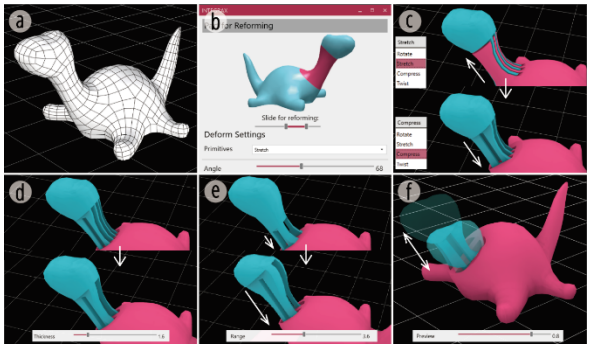

Figure 14: All-in-One Print workflow of designing.

5.1.2 DIY design for complicated and linked motions. For experts such as sophisticated makers or kinetic designers, the basic and separated motion modification tools may not fulfill their needs. Our pipeline also allows for further or full-course DIY designs for more complex and linked motions. To ensure that the designed components are printable, we provide the following seven instructions for users during the DIY process:

For components that do not attach to the platform:

- I1: The majority of the component should be situated between the shell or other parts (Figure 15a);
- I2: More than half of their bottoms should be parallel to the print platform, with the remaining parts at an angle greater than 35 degrees (Figure 15b);
- I3: Wall thickness should be larger than 1.5mm (Figure 15c).
- For large-span suspension structures:
- I4: Ensure that the bottom of the structure is parallel to the print bed (Figure 15d);

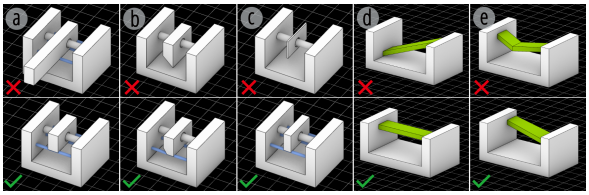

Figure 15: Instructions for DIY kinetic design.

- I5: Avoid the inclusion of complex shapes such as corners in suspension (Figure 15e);
- I6: Do not exceed the length of 10cm.

I1 ensures that the ends of the *Support-bridges* can be attached to other parts; I2 can prevent instability during the printing process and prevent initial shape oscillation caused by non-planar starting layers, while small angles can cause filament sagging; I3 can affect the print quality, and thin components can hardly be printable on the *Support-bridges*. I4 and I5 meet the basic logic of bridge-linked printing, allowing for the analysis of straight and long bridges by *Arch-printing*. Until now, we have not developed cross-layer bridge-linked printing; I6 is the longest stable *Arch-printing* distance tested by us, and the distance close to half the platform can meet most cases.

5.2 Analysis and G-code generation

Additionally, our system is capable of analyzing and generating *Support-bridges* and *Arch-printing* for input models. We clarify this step with examples of the result of our design tool (Figure 16b) and also a switch model [48] (Figure 16a) downloaded from Thingivers [35] as an output of the DIY process.

The first step is collision detection and elimination. Due to the limited accuracy of the printer, we will offset each individual part by 0.3 mm. If there are overlapping parts (Figure 16a2), we will perform a Boolean operation to remove parts prone to adhesion during printing. Afterward, for components that do not attach to the platform, we will analyze the orientation of all mesh faces (see Section 3.2.1 for rules) and generate *Support-bridges* with a unit length extrusion amount of e=1.2 and a speed of 20 mm/s, along with the starting and ending positions. We record them in the format of G1 as {B}. Such parameters can ensure the toughness and support of *Support-bridges*.

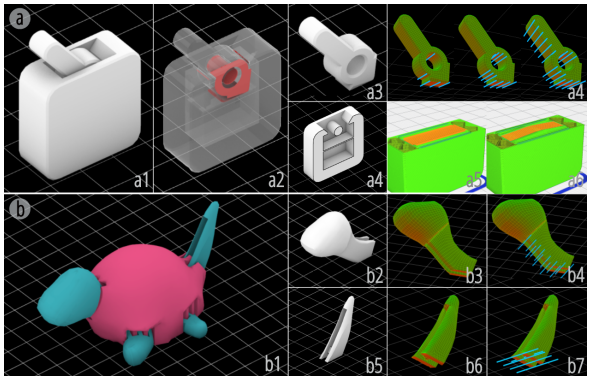

Figure 16: The process of G-code generation with Support-bridges and Arch-printing.

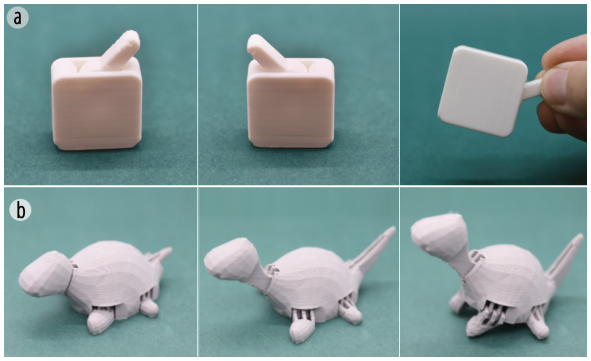

Figure 17: Integrated well-printed object after All-in-One Print.

To avoid redundant options in our system and following bugs, we edit the G-code from users' slicing software (Cura, S3d, etc.) with customized settings. For example, for *Support-bridges* {B}, according to the z coordinates, our software will automatically weave them inside at the end of the corresponding layer. For *Arch-printing*, the system will filter out G1 with a span greater than 25 mm and no printing beneath. It will then insert five coordinates with higher z coordinates in the middle to approximate the arctangent function (Section 3.1.2) and adjust the extrusion amount to e=1.1 and the speed to 15 mm/s.

At this point, all G-code adjustments can be well-printed to produce results containing *Arch-printing* and removable *Support-bridges*. Figure 17 shows the printed result through the pipeline for the print-at-one-go paradigm.

6 APPLICATIONS

The none-assembly production process significantly saves the manual effort of the following applications. One single print job could even achieve multiple kinetic prints directly for usage. Their robustness is also enhanced by the absence of gaps and connections in the shells, which are inevitable in the conventional print-assemble method. Thus, most manual deformations and even drops at human height can hardly cause any breakage.

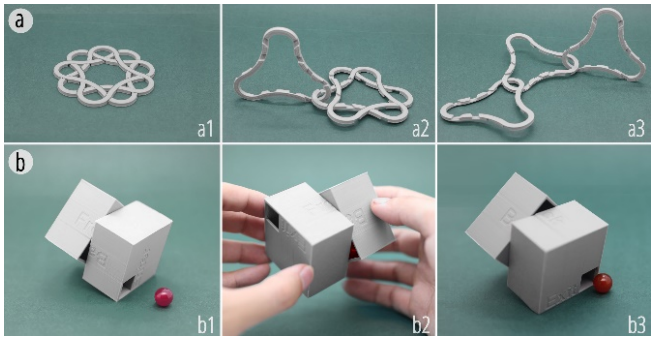

Figure 18: Puzzle with arch bridges printed for solving.

6.1 Puzzles

Puzzles are one of the most popular models in the maker community. However, the individual components of most puzzles need to be printed separately and then assembled. This process inevitably makes users aware of the internal structures, which spoils the enjoyment of solving and exploring the final puzzle.

All-in-One Print offers a unique experience by providing fully assembled components. In addition, the unknown internal content adds to the challenge and enjoyment of the puzzle. We have designed a rotatable box with a complex internal void. To maintain the integrity of the void, *Arch-printing* is used for the cross (Figure 18a) and roof (Figure 18b) printing. The puzzle contains a three-dimensional maze, which is hidden from the user. The objective is to orient the puzzle in a sequence of maneuvers so that the marble can travel between the entrance and exit. Without having access to its internal, users must rely on hearing and feeling the marble's movement as it travels through the cavity.

6.2 Animal toys

In the hedgehog and jellyfish designs (Figure 19), we used a design tool to achieve simple motions through design tools and then further linked them manually. In the design process, a modification design tool is used for the basic stretch motion of the jellyfish body and rotate motion for the tentacles. After replacing the blue part with six tentacles, we set 0.7 mm for collision detection and elimination to have a loose and sagging property that allows the tentacles to swing with manual movement or even gentle wind.

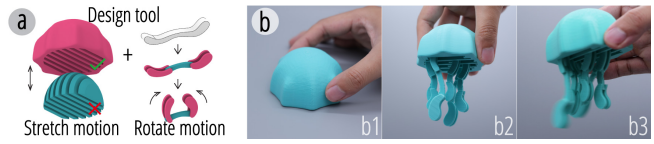

Figure 19: A jellyfish with six tentacles, each consisting of 3 joints.

In the hedgehog design (Figure 20), the software generated the compressing structure of the hedgehog body and then manually modeled the rotating 22 spikes and designed the connecting parts to achieve the linkage of the mechanism. By using *Support-bridges* to support each spine, we were able to ensure high-quality printing

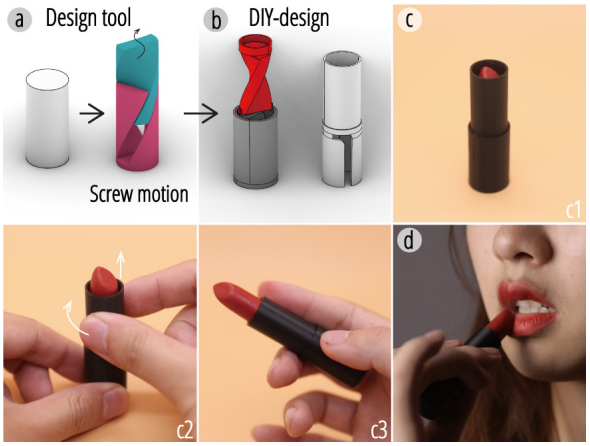

Figure 21: (a) Exploded drawing of the lipstick with extra design on Screwing primitive; (b) A integrated printed lipstick added with DIY lipstick cream; (c-d) Usage Scenarios.

and strengthen the connection between components. To mimic the behavior of a hedgehog when it is frightened, the slide motion of the body allows its head to retract with all spines standing up in a defensive stance.

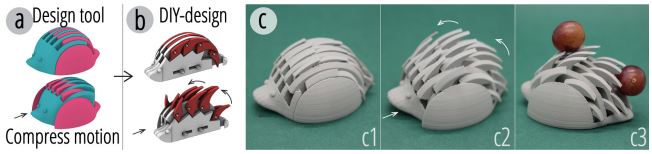

Figure 20: A printed hedgehog with 22 retractable spines, realized by rotational linkages.

6.3 Daily-life objects

In addition to single deformation behavior, integrated fabrication of multiple interactive deformations allows user input conversion into motion. For example, the design of conventional lipstick typically consists of various parts, including a container of cream, an outer tube, a liftable base, two inner bars, and exterior walls. We have combined all these structures into a single, integrated print (Figure 21b). This device converts the user's motions of rotating the body into lifting the cream container. With a printing layer height of 0.06 mm and ironing, the lifting motion is smooth, and the final state is maintained even with 25 degrees of over-rotation.

6.4 Number Pad and MIDI Keyboard

We design and build a number pad using our method. We use the standard key layout, which includes 19 squared keys. *Support-bridges* are implemented between key caps and keyframes to offer support and stabilization throughout the printing. The advantage of our integrated printing is that we can take full control of the internal design. Thus, we can modify the profile of the spring fins to adjust the tactile strength of the key, as shown in Figure 22a. To convert the external input to an electrical signal, we salvage the

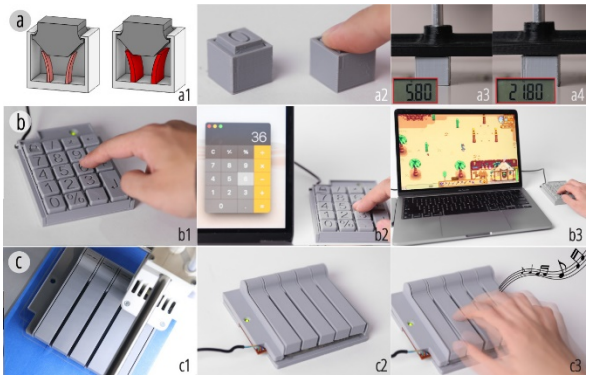

Figure 22: (a) Two movement of the character, with the help of key binding settings. Buttons modified with elastic walls of different thicknesses and lengths for different haptic feedback; (b) An All-in-One number pad printed with less resilience; (c) A wide MIDI keyboard with remarkable re-silience.

PCB and dome switches mesh from a discarded number pad and place it underneath the frame and the keys.

Similarly, we also design and build a MIDI keyboard with five keys. By connecting it to a laptop in Figure 22, the number pad could be used to calculate and control the movement of the in-game character. In Figure 22c, the 5-key MIDI keyboard functions as a piece of instrument, providing similar tactile feedback as that of the commercially available keyboard.

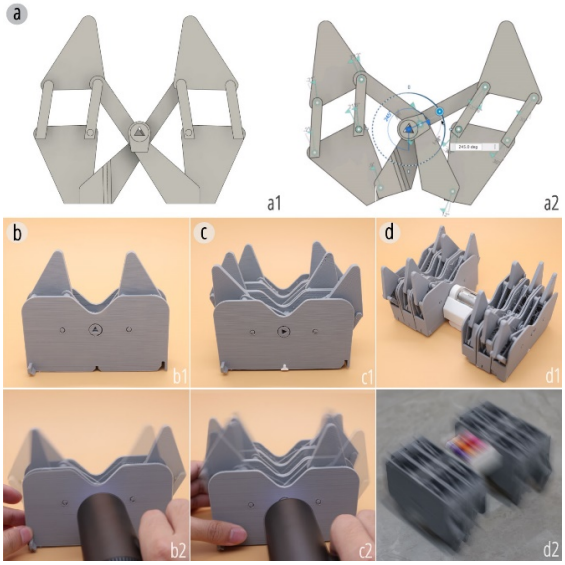

Figure 23: (a) A kinematic design of Strandbeest with the simulation of mechanical motions; (b) All-in-One Print result of a pair of legs driven with a power drill; (c) Three pairs of legs linked together with one-third of the pace difference; (d) Final result of the Strandbeest walking on the ground.

6.5 Strandbeest

Strandbeest (Figure 23) is a human-scale walking kinetic sculpture that Theo Jansen invented in 1990. Its intricate linkages make it a great example to showcase the capability of our integrated printing method. However, the challenge in fabricating Strandbeest is the six pairs of legs with 256 components in total and removing support and fixing matching errors, which may occur throughout the printing. Compared to the conventional print-assemble method, the All-in-one Print method eliminates the need for assembly and post-processing and significantly reduces the total print time. In addition, to increase the success rate, the density of the *Support-bridges* was parametrically tuned beyond average to minimize the vibrations in the printing process.

7 EVALUATION

7.1 Overview

7.1.1 Models preparation. To evaluate our approach, comparing printed-assembled objects and All-in-One Print objects become necessary. For better qualities of printed-assembled objects, we adopted three models from Thingivers[48, 50, 51], which were designed by expert makers. To ensure their feasibility, we selected the models based on the following criteria: (1) high number of downloads and likes; (2) covering most of the joints (rotate, slide, and ball joint) mentioned in this paper; (3) meets the six instructions standards (Section 5.1.2).

For the All-in-One Print models, they should go through the pipeline of DIY-designed models. Thus, we took the six instructions as a starting point to adjust the models virtually. Some details were handled manually, such as flatting the bottom of the separated part and modifying the inclination of some surfaces. We ensured that all adjustments were within 1.0 mm. These operations were done to ensure that *Support-bridges* and *Arch-printing* could be generated correctly. After that, we import them for collision detection and G-code generation. Both print files have identical settings (layer height 0.2 mm, speed 70 mm/s, infill 10%, without adhesion and support).

7.1.2 Users. We conducted a user study to obtain feedback on the post-processing process and the final objects. In this user study, we gathered eight participants, four males, and four females, all aged between 21 to 50 years old. Four participants had no prior experience with 3D printing, handicrafts, or digital fabrication; two had no experience with digital fabrication but had rich experience with handicrafts.; the remaining two had rich experience in both areas.

We divided the participants into two groups: the novice group (consisting of the first four participants) and the experienced group (consisting of the latter four participants). They went through the same process but were evaluated separately during the assessment. Each individual was compensated approximately $15 equivalent to the local currency for participation.

7.2 Procedure

During each evaluation session, participants were presented with three groups of components made with the conventional print-assemble method and three integrated prints with the All-in-One Print method. In addition, the participants were tasked with the following:

User Experience	
Q1.[Difficulty]	Post-process is technically difficult to you
Q2.[Appearance]	You like the object's appearance after post-process
Q3.[Efficiency]	The post-process is efficient
Q4.[Frustration]	You feel frustration in post-process
Usability	
Q5.[Motion Flexibility]	The result is easy to deform
Q6.[Motion Range]	The result could be deformed in large range
Q7.[Function Robustness]	The result is hard to be disassemble or broken

Figure 24: Questionnaires.

Study on the user experience of manual fabrication:

- They were given brief instructions on the design and fabrication process of the products.
- They manually assembled the three printed-assemble products, and the assembly time was recorded.
- They manually removed the *Support-bridges* of the 3 All-in-One Print products to make them flexible, and the time was recorded.
- They completed a questionnaire on their experience with manual fabrication.

Study on the user experience with the mechanical structures:

- They manipulated the joints of all the assembled objects with kinetic structures.
- They completed a questionnaire on their experience with the kinetic structures.
- We conducted a semi-structured interview based on their answers to the questionnaire.

7.3 Results

The results of Q1 [Difficulty] show that our proposed method significantly decreased the difficulty of the post-processing process, particularly for complex printed-assembled objects. Using the All-in-One Print method reduced the difficulty level from 3.83 to 1.25 in the novice group and 2.5 to 1 in the experienced group.

The results of Q2 [Appearance] show that experienced participants reported increased satisfaction with the appearance of All-in-One Printed products compared to printed-assembled products (from 3.08 to 4.08) in most cases. Overall, the experienced group reported slightly higher satisfaction with the appearance of All-in-One Printed products.

Looking at the result of Q3 [Efficiency] and Q4 [Frustration], participants found that the efficiency of the All-in-One Printed products was very significant (novice group from 1.67 to 4.75, experienced group from 2.5 to 4.92). Accordingly, although the finished product drawings were available for reference during the assembly of printed-assembled products, confusion, and uncertainty still arose during the assembly process. Additionally, many parts required additional tools, such as pliers and files, due to matching errors, resulting in increased difficulty in assembly.

Novice users found that the All-in-One Printed products had significant advantages in terms of completion speed and finished product quality (Q7), giving scores above 4.0. Printed-assembled

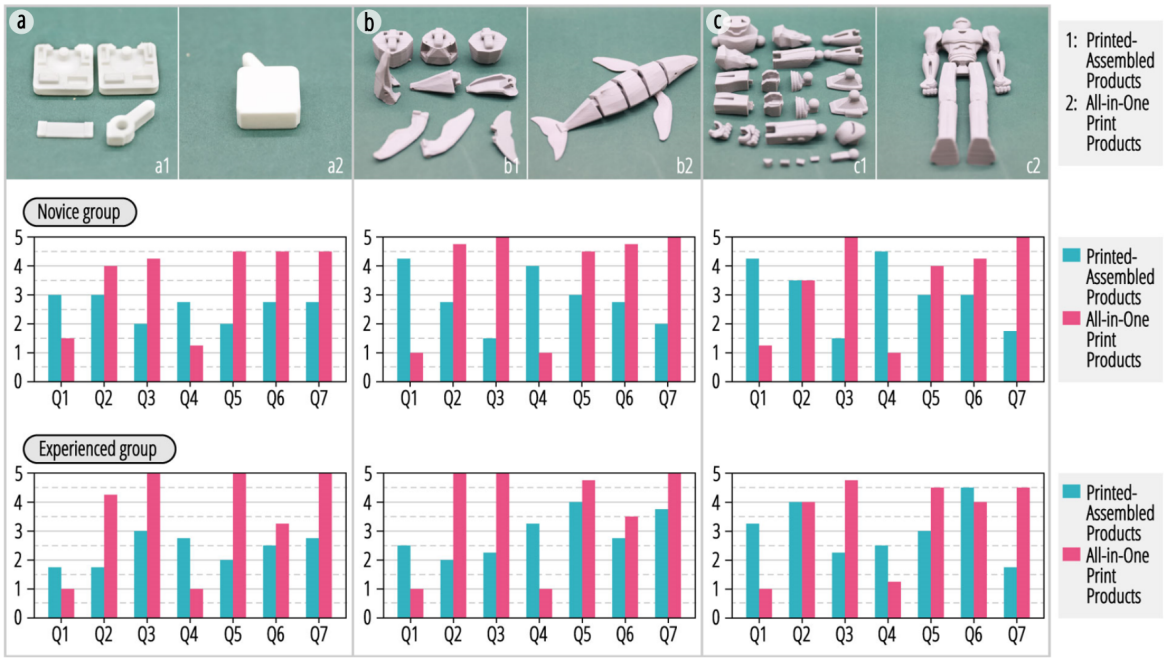

Figure 25: The sores from novices and experienced groups of the (a)switch, (b)whale, and (c)robot in response to the questionnaire.

items were more likely to disassemble or break during the manipulation, while this rarely happened with the All-in-One Printed products. The experienced group found that, after considering usability and stability (Q5, Q6, Q7), the kinetic performance of All-in-One Print products was better in the Switch and Whale cases. However, experienced users also scored the Robot All-in-One Printed products negatively on Q5[Motion Flexibility], stating that they felt the Robot case should have required some friction to maintain the postures, but those All-in-One Printed products felt too loose. They also provided suggestions for improving workflow efficiency and printing quality, which are discussed in the Discussion and Future Work sections.

8 LIMITATION AND FUTURE WORK

8.1 Shell requirement for All-in-One Print

A printable *Support-bridges* must be attached to other objects at both ends, which can be challenging in cases where there are no shells or walls on both sides. To address this issue, we always ensure that part of the blue component is surrounded by the pink component during the All-in-One Print generation process (Figure 13b-f), which facilitates the generation of *Support-bridges*. In general, suspension bridges can only be completed with supports at either end and cannot replace conventional support in all cases.

8.2 Iteration cycles

While All-in-One Print can accelerate manufacturing and reduce assembly time during the final fabrication stage, the design and iteration process can be challenging. Manual modeling, printing, and modifications can be time-consuming, and a failed print of a single part can render the entire product obsolete. That's why we have designed Strandbeest modularly. Over the course of multiple iterations, we have not only improved the product's design but also refined the All-in-One Print system. We have developed gap thicknesses and bridges to prevent shaking and have constantly updated our default settings to improve the success rate of printing. While there is still work to be done in this area, our experience in the design process has directly informed the development of our design tools. We plan to make the design tool web-based in future work for further accessibility with All-in-One Print.

8.3 Excessive Support-bridges

In most cases, the *Support-bridges* can be easily removed with simple motions. However, they can also be removed manually for aesthetic purposes. Additionally, multiple *support-bridges* will be automatically generated for large-scale prints to ensure print quality as the size of each component increases. In some cases, however, the input motions fail to provide enough force to remove every bridge, particularly for components with laborious lever capabilities. For such, individual tensions need to be applied to each component for removal, and post-processing is required to remove the *Support-bridges* using tools.

8.4 Multi-stable structure for Ball joint

In our design, we propose several multi-stable All-in-One Print designs (Figure 8) that can achieve multi-stable structures of single-degree-of-freedom for rotating and stretching prototypes. However, our exploration of multi-stable systems in a higher degree of freedom is limited.

We used the All-in-One Print method to reproduce the ball-joint structure. Our approach enhanced the integrity and robustness of

the original ball-joint products. However, due to the gaps reserved for printers' inaccuracy, it did not well reproduce their inherent physical properties of them (friction and stabilities).

In the future, based on the multi-stable structure with a single degree of freedom, we will explore using polyhedrons instead of a sphere and extend the design space for multi-stable ball joints.

8.5 Further integration with All-in-One Print.

Printing integrated circuits is a widespread application in the field of HCI fabrication [21], etc. While flattened circuits are commonly used, our goal is to create integrated circuits using unique fabrication with FDM printers. This involves modifying the print head and G-code control to inject conductive material into gaps reserved in 3D-printed objects automatically. This is a challenging but inspiring and meaningful area of research. In the future, we plan to explore the integration of non-assemblies with other materials, existing components, or sensors, which could enable the creation of smart All-in-One Prints by integrating these components midway through the manufacturing process.

9 CONCLUSION

In this work, we have demonstrated that the All-in-One Print objects' design tool and fabrication method can integrate multiple kinematic mechanisms into one object with a consumer-grade 3D printer. Compared with multiple steps of the conventional process, including manufacturing separated components, post-processing, and assembling, we present non-assembly All-in-One Print integrated with multiple deformation primitives, stability control, and continuous creation in an active way. We developed a computational design tool to create integrated prints, which can be directly 3D printed and easily deformed afterward. Furthermore, we also demonstrate various application cases, including toys with interactive aesthetics and daily items with internalized functions. We look forward to extending our method into future sustainable fabrication.

ACKNOWLEDGMENTS

This project is supported by the National Natural Science Foundation of China (No. 62202423), the Fundamental Research Funds for the Central Universities (No. 2022FZZX01-22), and the Zhejiang – Singapore Innovation and AI Joint Research Lab.

Our sincere appreciation to Ziyao Chen, Xiaoyu Ge, Lingchuan Zhou and Shanghua Lou, whose work inspired and helped us a lot.

REFERENCES

[1] Muhammad Abdullah, Romeo Sommerfeld, Laurenz Seidel, Jonas Noack, Ran Zhang, Thijs Roumen, and Patrick Baudisch. 2021. Roadkill: Nesting Laser-Cut Objects for Fast Assembly. In *The 34th Annual ACM Symposium on User Interface Software and Technology*, ACM, Virtual Event USA, 972–984. DOI:https://doi.org/10.1145/3472749.3474799

[2] Davide Jose Nogueira Amorim, Troy Nachtigall, and Miguel Bruns Alonso. 2019. Exploring mechanical meta-material structures through personalised shoe sole design. In *Proceedings of the ACM Symposium on Computational Fabrication*, ACM, Pittsburgh Pennsylvania, 1–8. DOI:https://doi.org/10.1145/3328939.3329001

[3] Moritz Bächer, Bernd Bickel, Doug L. James, and Hanspeter Pfister. 2012. Fabricating articulated characters from skinned meshes. *ACM Trans. Graph.* 31, 4 (August 2012), 1–9. DOI:https://doi.org/10.1145/2185520.2185543

[4] M Beecroft. 2016. 3D printing of weft knitted textile based structures by selective laser sintering of nylon powder. *IOP Conf. Ser. Mater. Sci. Eng.* 137, (July 2016), 012017. DOI:https://doi.org/10.1088/1757-899X/137/1/012017

[5] Franklin Pezzuti Dyer and Leah Buechley. 2022. Extruder-Turtle: A Library for 3D Printing Delicate, Textured, and Flexible Objects. (2022), 9.

[6] Jack Forman, Mustafa Doga Dogan, Hamilton Forsythe, and Hiroshi Ishii. 2020. DefeXtiles: 3D Printing Quasi-Woven Fabric via Under-Extrusion. In *Proceedings of the 33rd Annual ACM Symposium on User Interface Software and Technology*, ACM, Virtual Event USA, 1222–1233. DOI:https://doi.org/10.1145/3379337.3415876

[7] Jun Gong, Olivia Seow, Cedric Honnet, Jack Forman, and Stefanie Mueller. 2021. MetaSense: Integrating Sensing Capabilities into Mechanical Metamaterial. In *The 34th Annual ACM Symposium on User Interface Software and Technology*, ACM, Virtual Event USA, 1063–1073. DOI:https://doi.org/10.1145/3472749.3474806

[8] Jianzhe Gu, Yuyu Lin, Qiang Cui, Xiaoqian Li, Jiaji Li, Lingyun Sun, Cheng Yao, Fangtian Ying, Guanyun Wang, and Lining Yao. 2022. PneuMesh: Pneumatic-driven Truss-based Shape Changing System. In *CHI Conference on Human Factors in Computing Systems*, ACM, New Orleans LA USA, 1–12. DOI:https://doi.org/10.1145/3491102.3502099

[9] Liang He, Huaishu Peng, Michelle Lin, Ravikanth Konjeti, François Guimbretière, and Jon E. Froehlich. 2019. Ondulé: Designing and Controlling 3D Printable Springs. In *Proceedings of the 32nd Annual ACM Symposium on User Interface Software and Technology*, ACM, New Orleans LA USA, 739–750. DOI:https://doi.org/10.1145/3332165.3347951

[10] Yunwoo Jeong, Han-Jong Kim, and Tek-Jin Nam. 2018. Mechanism Perfboard: An Augmented Reality Environment for Linkage Mechanism Design and Fabrication. In *Proceedings of the 2018 CHI Conference on Human Factors in Computing Systems*, ACM, Montreal QC Canada, 1–11. DOI:https://doi.org/10.1145/3173574.3173985

[11] Jingchao Jiang, Jonathan Stringer, and Xun Xu. Support Optimization for Flat Features via Path Planning in Additive Manufacturing. 9.

[12] Han-Jong Kim, Yunwoo Jeong, Ju-Whan Kim, and Tek-Jin Nam. 2018. A prototyping tool for kinetic mechanism design and fabrication: Developing and deploying M.Sketch for science, technology, engineering, the arts, and mathematics education. *Adv. Mech. Eng.* 10, 12 (December 2018), 168781401880410. DOI:https://doi.org/10.1177/1687814018804104

[13] Robert Kovacs, Lukas Rambold, Lukas Fritzsche, Dominik Meier, Jotaro Shigeyama, Shohei Katakura, Ran Zhang, and Patrick Baudisch. 2021. Trusscillator: a System for Fabricating Human-Scale Human-Powered Oscillating Devices. In *The 34th Annual ACM Symposium on User Interface Software and Technology*, ACM, Virtual Event USA, 1074–1088. DOI:https://doi.org/10.1145/3472749.3474807

[14] Nianlong Li, Han-Jong Kim, LuYao Shen, Feng Tian, Teng Han, Xing-Dong Yang, and Tek-Jin Nam. 2020. HapLinkage: Prototyping Haptic Proxies for Virtual Hand Tools Using Linkage Mechanism. In *Proceedings of the 33rd Annual ACM Symposium on User Interface Software and Technology*, ACM, Virtual Event USA, 1261–1274. DOI:https://doi.org/10.1145/3379337.3415812

[15] Hongnan Lin, Liang He, Fangli Song, Yifan Li, Tingyu Cheng, Clement Zheng, Wei Wang, and HyunJoo Oh. 2022. FlexHaptics: A Design Method for Passive Haptic Inputs Using Planar Compliant Structures. In *CHI Conference on Human Factors in Computing Systems*, ACM, New Orleans LA USA, 1–13. DOI:https://doi.org/10.1145/3491102.3502113

[16] Vittorio Megaro, Jonas Zehnder, Moritz Bächer, Stelian Coros, Markus Gross, and Bernhard Thomaszewski. A Computational Design Tool for Compliant Mechanisms. *ACM Trans. Graph.* 36, 4 , 12.

[17] Ioanna Mitropoulou, Mathias Bernhard, and Benjamin Dillenburger. 2020. Print Paths Key-framing: Design for non-planar layered robotic FDM printing. In *Symposium on Computational Fabrication*, ACM, Virtual Event USA, 1–10. DOI:https://doi.org/10.1145/3424630.3425408

[18] Ken Nakagaki, Artem Dementyev, Sean Follmer, Joseph A. Paradiso, and Hiroshi Ishii. 2016. ChainFORM: A Linear Integrated Modular Hardware System for Shape Changing Interfaces. In *Proceedings of the 29th Annual Symposium on User Interface Software and Technology*, ACM, Tokyo Japan, 87–96. DOI:https://doi.org/10.1145/2984511.2984587

[19] Ken Nakagaki, Joanne Leong, Jordan L. Tappa, João Wilbert, and Hiroshi Ishii. 2020. HERMITS: Dynamically Reconfiguring the Interactivity of Self-propelled TUIs with Mechanical Shell Add-ons. In *Proceedings of the 33rd Annual ACM Symposium on User Interface Software and Technology*, ACM, Virtual Event USA, 882–896. DOI:https://doi.org/10.1145/3379337.3415831

[20] Ken Nakagaki, Luke Vink, Jared Counts, Daniel Windham, Daniel Leithinger, Sean Follmer, and Hiroshi Ishii. 2016. Materiable: Rendering Dynamic Material Properties in Response to Direct Physical Touch with Shape Changing Interfaces. In *Proceedings of the 2016 CHI Conference on Human Factors in Computing Systems*, ACM, San Jose California USA, 2764–2772. DOI:https://doi.org/10.1145/2858036.2858104

[21] Martin Nisser, Christina Chen Liao, Yuchen Chai, Aradhana Adhikari, Steve Hodges, and Stefanie Mueller. 2021. LaserFactory: A Laser Cutter-based Electromechanical Assembly and Fabrication Platform to Make Functional Devices & Robots. In *Proceedings of the 2021 CHI Conference on Human Factors in Computing Systems*, ACM, Yokohama Japan, 1–15. DOI:https://doi.org/10.1145/3411764.3445692

[22] Yuta Noma, Koya Narumi, Fuminori Okuya, and Yoshihiro Kawahara. 2020. Pop-up Print: Rapidly 3D Printing Mechanically Reversible Objects in the Folded State.

In *Proceedings of the 33rd Annual ACM Symposium on User Interface Software and Technology*, ACM, Virtual Event USA, 58–70. DOI:https://doi.org/10.1145/3379337.3415853

[23] Keunwoo Park, Conrad Lempert, Muhammad Abdullah, Shohei Katakura, Jotaro Shigeyama, Thijs Roumen, and Patrick Baudisch. 2022. FoolProofJoint: Reducing Assembly Errors of Laser Cut 3D Models by Means of Custom Joint Patterns. In *CHI Conference on Human Factors in Computing Systems*, ACM, New Orleans LA USA, 1–12. DOI:https://doi.org/10.1145/3491102.3501919

[24] Amanda J. Parkes, Hayes Solos Raffle, and Hiroshi Ishii. 2008. Topobo in the wild: longitudinal evaluations of educators appropriating a tangible interface. In *Proceeding of the twenty-sixth annual CHI conference on Human factors in computing systems - CHI '08*, ACM Press, Florence, Italy, 1129. DOI:https://doi.org/10.1145/1357054.1357232

[25] Katy Pieri, Bailey M. Felix, Teng Zhang, Pranav Soman, and James H. Henderson. 2021. Printing Parameters of Fused Filament Fabrication Affect Key Properties of Four-Dimensional Printed Shape-Memory Polymers. *3D Print. Addit. Manuf.* (October 2021), 3dp.2021.0072. DOI:https://doi.org/10.1089/3dp.2021.0072

[26] Stefan Pillwein, Johanna Kübert, Florian Rist, and Przemyslaw Musialski. 2020. Design and Fabrication of Elastic Geodesic Grid Structures. In *Symposium on Computational Fabrication*, 1–11. DOI:https://doi.org/10.1145/3424630.3425412

[27] Michael L. Rivera and Scott E. Hudson. 2019. Desktop Electrospinning: A Single Extruder 3D Printer for Producing Rigid Plastic and Electrospun Textiles. In *Proceedings of the 2019 CHI Conference on Human Factors in Computing Systems*, ACM, Glasgow Scotland Uk, 1–12. DOI:https://doi.org/10.1145/3290605.3300434

[28] Thijs Roumen, Yannis Kommana, Ingo Apel, Conrad Lempert, Markus Brand, Erik Brendel, Laurenz Seidel, Lukas Rambold, Carl Goedecken, Pascal Crenzin, Ben Hurdelhey, Muhammad Abdullah, and Patrick Baudisch. 2021. Assembler3: 3D Reconstruction of Laser-Cut Models. In *Proceedings of the 2021 CHI Conference on Human Factors in Computing Systems*, ACM, Yokohama Japan, 1–11. DOI:https://doi.org/10.1145/3411764.3445453

[29] Thijs Roumen, Conrad Lempert, Ingo Apel, Erik Brendel, Markus Brand, Laurenz Seidel, Lukas Rambold, and Patrick Baudisch. 2021. autoAssembler: Automatic Reconstruction of Laser-Cut 3D Models. In *The 34th Annual ACM Symposium on User Interface Software and Technology*, ACM, Virtual Event USA, 652–662. DOI:https://doi.org/10.1145/3472749.3474776

[30] Christian Schumacher, Bernd Bickel, Jan Rys, Steve Marschner, Chiara Daraio, and Markus Gross. 2015. Microstructures to control elasticity in 3D printing. *ACM Trans. Graph.* 34, 4 (July 2015), 1–13. DOI:https://doi.org/10.1145/2766926

[31] Katherine W Song and Eric Paulos. 2021. Unmaking: Enabling and Celebrating the Creative Material of Failure, Destruction, Decay, and Deformation. In *Proceedings of the 2021 CHI Conference on Human Factors in Computing Systems*, ACM, Yokohama Japan, 1–12. DOI:https://doi.org/10.1145/3411764.3445529

[32] Lingyun Sun, Jiaji Li, Yu Chen, Yue Yang, Zhi Yu, Danli Luo, Jianzhe Gu, Lining Yao, Ye Tao, and Guanyun Wang. 2021. FlexTruss: A Computational Threading Method for Multi-material, Multi-form and Multi-use Prototyping. In *Proceedings of the 2021 CHI Conference on Human Factors in Computing Systems* (CHI '21), Association for Computing Machinery, New York, NY, USA, 1–12. DOI:https://doi.org/10.1145/3411764.3445311

[33] Haruki Takahashi and Jeeeun Kim. 2019. 3D Printed Fabric: Techniques for Design and 3D Weaving Programmable Textiles. In *Proceedings of the 32nd Annual ACM Symposium on User Interface Software and Technology*, ACM, New Orleans LA USA, 43–51. DOI:https://doi.org/10.1145/3332165.3347896

[34] Thingiverse.com. 2019. Chainmail - 3D Printable Fabric by flowalistik. Retrieved September 16, 2022 from https://www.thingiverse.com/thing:3096598

[35] Thingiverse.com. Thingiverse - Digital Designs for Physical Objects. Retrieved September 16, 2022 from https://www.thingiverse.com/

[36] Bernhard Thomaszewski, Stelian Coros, Damien Gauge, Vittorio Megaro, Eitan Grinspun, and Markus Gross. 2014. Computational design of linkage-based characters. *ACM Trans. Graph.* 33, 4 (July 2014), 1–9. DOI:https://doi.org/10.1145/2601097.2601143

[37] Thibault Tricard, Vincent Tavernier, Cédric Zanni, Jonàs Martínez, Pierre-Alexandre Hugron, Fabrice Neyret, and Sylvain Lefebvre. 2020. Freely orientable microstructures for designing deformable 3D prints. *ACM Trans. Graph.* 39, 6 (December 2020), 1–16. DOI:https://doi.org/10.1145/3414685.3417790

[38] Yongqiang Tu, Javier A. Arrieta-Escobar, Alaa Hassan, Uzair Khaleeq uz Zaman, Ali Siadat, and Gongliu Yang. 2021. Optimizing Process Parameters of Direct Ink Writing for Dimensional Accuracy of Printed Layers. *3D Print. Addit. Manuf.* (December 2021), 3dp.2021.0208. DOI:https://doi.org/10.1089/3dp.2021.0208

[39] Guanyun Wang, Ye Tao, Ozguc Bertug Capunaman, Humphrey Yang, and Lining Yao. 2019. A-line: 4D Printing Morphing Linear Composite Structures. In *Proceedings of the 2019 CHI Conference on Human Factors in Computing Systems*, ACM, Glasgow Scotland Uk, 1–12. DOI:https://doi.org/10.1145/3290605.3300656

[40] Guanyun Wang, Humphrey Yang, Zeyu Yan, Nurcan Gecer Ulu, Ye Tao, Jianzhe Gu, Levent Burak Kara, and Lining Yao. 2018. 4DMesh: 4D Printing Morphing Non-Developable Mesh Surfaces. In *Proceedings of the 31st Annual ACM Symposium on User Interface Software and Technology*, ACM, Berlin Germany, 623–635. DOI:https://doi.org/10.1145/3242587.3242625

[41] Christopher Yu, Keenan Crane, and Stelian Coros. 2017. Computational design of telescoping structures. *ACM Trans. Graph.* 36, 4 (July 2017), 1–9. DOI:https://doi.org/10.1145/3072959.3073673

[42] Grasshopper - algorithmic modeling for Rhino. Retrieved September 16, 2022 from https://www.grasshopper3d.com/

[43] <number>[43]</number>Lingyun Sun, Jiaji Li, Junzhe Ji, Deying Pan, Mingming Li, Kuangqi Zhu, Yitao Fan, Yue Yang, Ye Tao, and Guanyun Wang. 2022. X-Bridges: Designing Tunable Bridges to Enrich 3D Printed Objects' Deformation and Stiffness. In Proceedings of the 35th Annual ACM Symposium on User Interface Software and Technology (UIST '22). Association for Computing Machinery, New York, NY, USA, Article 20, 1–12. DOI:https://doi.org/10.1145/3526113.3545710

[44] Blair Subbaraman and Nadya Peek. 2022. P5.fab: Direct Control of Digital Fabrication Machines from a Creative Coding Environment. In Designing Interactive Systems Conference (DIS '22). Association for Computing Machinery, New York, NY, USA, 1148–1161. DOI:https://doi.org/10.1145/3532106.3533496

[45] Jacques Calì, Dan A. Calian, Cristina Amati, Rebecca Kleinberger, Anthony Steed, Jan Kautz, and Tim Weyrich. 2012. 3D-printing of non-assembly, articulated models. ACM Trans. Graph. 31, 6, Article 130 (November 2012), 8 pages. DOI:https://doi.org/10.1145/2366145.2366149

[46] A. G. Ambekar. 2007. Mechanism and machine theory. PHI Learning Private Limited, Delhi.

[47] Frikk Fossdal, Rogardt Heldal, and Nadya Peek. 2021. Interactive Digital Fabrication Machine Control Directly Within a CAD Environment. In Proceedings of the 6th Annual ACM Symposium on Computational Fabrication (SCF '21). Association for Computing Machinery, New York, NY, USA, Article 8, 1–15. DOI:https://doi.org/10.1145/3485114.3485120

[48] Fidget Toggle Switch- Digital Designs by kriswillcode November 20, 2021 from https://www.thingiverse.com/thing:5141239/comments

[49] Stefanie Mueller, Bastian Kruck, and Patrick Baudisch. 2013. LaserOrigami: laser-cutting 3D objects. In CHI '13 Extended Abstracts on Human Factors in Computing Systems (CHI EA '13). Association for Computing Machinery, New York, NY, USA, 2851–2852. https://doi.org/10.1145/2468356.2479544

[50] Save the Whales (Kinetic Whales) by erwoong October 26, 2019 from https://www.thingiverse.com/thing:3934354

[51] Articulated armor robot by SebTheis September 09, 2016 from https://www.thingiverse.com/thing:1760622

[52] Lingyun Sun, Jiaji Li, Mingming Li, Yitao Fan, Yu Chen, Deying Pan, Yue Yang, Junzhe Ji, Ye Tao, and Guanyun Wang. 2021. 3DP-Ori: Bridging-Printing Based Origami Fabrication Method with Modifiable Haptic properties. In Adjunct Proceedings of the 34th Annual ACM Symposium on User Interface Software and Technology (UIST '21 Adjunct). Association for Computing Machinery, New York, NY, USA, 74–77. https://doi.org/10.1145/3474349.3480233

[53] Lingyun Sun, Yu Chen, Deying Pan, Yue Yang, Yitao Fan, Jiaji Li, Ziqian Shao, Ye Tao, and Guanyun Wang. 2021. FlexCube: 3D Printing Tunable Meta-structures with Triply Periodic Minimal Surfaces. In Extended Abstracts of the 2021 CHI Conference on Human Factors in Computing Systems (CHI EA '21). Association for Computing Machinery, New York, NY, USA, Article 190, 1–4. https://doi.org/10.1145/3411763.3451562

[54] Liang He, Xia Su, Huaishu Peng, Jeffrey Ian Lipton, and Jon E. Froehlich. 2022. Kinergy: Creating 3D Printable Motion using Embedded Kinetic Energy. In Proceedings of the 35th Annual ACM Symposium on User Interface Software and Technology (UIST '22). Association for Computing Machinery, New York, NY, USA, Article 69, 1–15. https://doi.org/10.1145/3526113.3545636

[55] Lingyun Sun, Jiaji Li, Yu Chen, Yue Yang, Ye Tao, Guanyun Wang, and Lining Yao. 2020. 4DTexture: A Shape-Changing Fabrication Method for 3D Surfaces with Texture. In Extended Abstracts of the 2020 CHI Conference on Human Factors in Computing Systems (CHI EA '20). Association for Computing Machinery, New York, NY, USA, 1–7. https://doi.org/10.1145/3334480.3383053

[56] Guanyun Wang, Tingyu Cheng, Youngwook Do, Humphrey Yang, Ye Tao, Jianzhe Gu, Byoungkwon An, and Lining Yao. 2018. Printed Paper Actuator: A Low-cost Reversible Actuation and Sensing Method for Shape Changing Interfaces. In Proceedings of the 2018 CHI Conference on Human Factors in Computing Systems (CHI '18). Association for Computing Machinery, New York, NY, USA, Paper 569, 1–12. https://doi.org/10.1145/3173574.3174143